

# The Global Ocean Conveyor Belt and the Southern Hemisphere Supergyre

Sabrina Speich\*‡, Bruno Blanke\* & Wenju Cai†

*\*Laboratoire de Physique des Océans, UMR 6523CNRS-IFREMER-UBO, Université de Bretagne Occidentale, UFR Sciences et Techniques, 6 avenue Le Gorgeu, 29238 Brest Cedex 3, France*

*†CSIRO Marine and Atmospheric Research, Private Bag No 1, Aspendale, Victoria 3195, Australia*

*‡ Present address: Institut de Recherche pour le Développement, Centre de Bretagne, Campus Ifremer, Technopole de Brest-Iroise - Site de la Pointe du Diable, 29280 Plouzané France.*

**The ocean's role in climate manifests itself through its high heat capacity, its own rich internal dynamics and its capability to transport heat and fresh-water<sup>1</sup> within the global ocean thermohaline circulation (THC)<sup>2</sup>. Because of the lack of observations, descriptions of the detailed circulation pathways have been difficult, and have been provided in terms of conceptual schemes<sup>3,4</sup>. Here, we establish the first quantitative, global three-dimensional picture of the THC using a Lagrangian reconstruction, which integrates hundreds of thousands of water parcel trajectories in a global ocean general circulation model. The resulting pattern enlightens the crucial role of the wind action in structuring the return flow to the North Atlantic. In particular, it reveals a strong link with the three subtropical gyres of the Southern Hemisphere (SH), which merge into a large three-ocean wide cell, referred to as the SH "supergyre". Because the THC pathways connect different regions of air-sea interaction, variations in their structure may influence the water masses they convey, and their associated heat and fresh-water transport.**

**This may induce large differences in the climate impact of the global ocean circulation. Therefore, the evidence that the “supergyre” plays a significant part in the THC has important implications for the understanding of the ocean’s role in the Earth climate and its changes.**

The THC is the large-scale ocean circulation driven by variations in density<sup>5</sup>. The structure of the associated mass fluxes has been conceptualized as the global Conveyor, which is the interconnected ocean currents associated with the North Atlantic overturning<sup>6</sup>. The North Atlantic surface-water cools, sinks, and flows southward as the North Atlantic Deep Water (NADW). Its structure and detailed connections with the rest of the World Ocean are particularly uncertain. Nevertheless, it is widely accepted that the Southern Ocean (SO) is a critical crossroad for this circulation, as it inter-connects the major basins, permitting the global THC, and providing an inter-ocean communication route for heat and freshwater anomalies<sup>7,8</sup>.

Over the last decade, several studies proposed a strong connection between the THC and tidal- and wind-energies<sup>9,10,11</sup>. Indeed, it is suggested that the overturn of the ocean must be accompanied by a SO upwelling of the deep water<sup>12</sup>. The presence of such upwelling is supported by numerous studies and some relate it to the wind forcing<sup>13,14</sup>. Winds are also responsible for at least a part of the meridional fluxes across the eastward flow of the Antarctic Circumpolar Current (ACC), which connects the SH polar region with the rest of the global ocean<sup>15</sup>. The physical structure of the Conveyor and its efficiency in climate regulation are therefore affected by the nature and the existence of these SO zonal and meridional exchanges through their influence on the involved water masses<sup>15</sup>. The lack of a comprehensive understanding of the detailed pathway of the Conveyor makes it difficult to assess the impact of such ocean processes

on the climate system.

Global ocean general circulation models (OGCMs), constrained to mimic observed tracer climatologies<sup>16</sup>, have been deployed to characterise some aspects of the three-dimensional (3-D) oceanic motion<sup>17</sup> using quantitative Lagrangian particle-following techniques. Here, we establish a global picture of the Conveyor from an extensive Lagrangian calculation of water parcel trajectories (see Methods). An objective circulation structure is obtained by calculating the 3-D non-divergent transport field established by the displacement of particles marked with an individual transport, and by computing the horizontal streamfunction associated with the vertical integration of this transport field. As a first 3-D quantitative visualization, Figure 1 shows the reconstructed pathways of the global Conveyor. To highlight both the deep and near surface routes, we drew only the “median” contour of the horizontal streamfunction. Colours represent the mean depth of the exchange between different key ocean sections. The numbers shown give the calculated mass transports for the corresponding coloured branch. The total transport associated with the model North Atlantic overturning is 17.4 Sv ( $1 \text{ Sv} = 10^6 \text{ m}^3 \text{ s}^{-1}$ ). The southward flowing NADW is replaced by 16.8 Sv of surface and thermocline waters coming from the South and by 0.6 Sv of Pacific water flowing across the Bering Strait.

Transformation of dense waters into upper-layer water takes place mainly in the SO during one or more circumnavigations of Antarctica, as discussed by previous studies<sup>13,14</sup>. When transformed these waters leak into the three SH oceanic basins, with the largest fraction penetrating into the Pacific Ocean. An amount of 5.2 Sv of NADW upwells and transforms into upper waters without flowing through the Passage of Drake. The rest, almost 12 Sv, recirculates mostly in the ACC and spreads within all

other ocean basins before coming back to the Atlantic, south of the African continent. The direct leakage of the Drake Passage water to the South Atlantic is less than 1 Sv and is not shown on Figure 1

The mean depths calculated along the various paths of the Conveyor upper branch show that the leakage of the circumpolar water to the Indian and Pacific subtropics occurs at different depths levels. The deepest path is located close to southern Australia and is related to the Tasman outflow<sup>18</sup>. Centred between 600 and 800 m, it subducts to approximately 1000 m en-route crossing the Indian Ocean. Once it reaches the Equatorial Atlantic, the path connected with the Tasman leakage carries the freshest and coolest waters of all routes (Fig. 2). Indeed, the Tasman outflow moves at a depth sufficiently isolated from the surface mixed layer where strong water mass transformations occur due to air-sea exchanges. The water has lower thermocline characteristics (Antarctic Intermediate Water and SubAntarctic Mode Water). As a result it is rather dense, and its bulk does not reach the surface except in the North Atlantic. The Tasman connection turns out to be the most efficient conveyor of low thermocline fresh water to feed into the North Atlantic. The major input of fresh, intermediate waters into the Atlantic Ocean occurs south of Africa. This result confirms previous findings<sup>19</sup> and is supported by a recent application of finite-difference inverse modelling to Atlantic hydrology and WOCE subsurface floats<sup>20</sup>.

The global Conveyor described above differs from the conventional pathways inferred from data analyses or inverse models<sup>7,21</sup>. For the North Atlantic return flow, the traditional pathway usually includes only two sources of water: the Indonesia Throughflow and the direct leakage to the South Atlantic from Drake Passage, respectively referred to as the “warm route” or “cold route”<sup>4</sup>. The usual estimated

partition is that the contribution from the Indonesian source lies around 6-8 Sv, whereas from the Drake Passage is  $\sim 10$  Sv. Our results contradict this view. While our reconstruction confirms the Indonesia Throughflow as a major provider of water for the North Atlantic return flow, it reduces the significance of the direct leakage from the Drake Passage and uncovers the Tasman outflow as a key feature in the global THC.

Because of its intermediate depth, the Tasman route has never been invoked before as a major global THC feature<sup>7,18,20</sup>, and it did not appear in the mean absolute dynamical topography recently derived<sup>22,23</sup>. Nevertheless, support of the existence of a Tasman Indo-Pacific connection can be found in ocean-tracer observations<sup>24,25</sup>, and in a recent compilation of the WOCE Indo-Pacific subsurface float data set<sup>26</sup>.

The structure of the Lagrangian derived streamfunction for the upper to intermediate layer waters associated with the North Atlantic overturning displays well organized features related to the large-scale wind forcing (Fig. 3). In particular, a subtropical “supergyre” spanning all three SH basins emerges. This large cell interconnects the three basins in two ways: i) a flow from west to east via its southern limit and parallel to the ACC, and ii) from east to west via its two northern branches: one through the Indonesian passages and the other confined to the South Pacific, which veers westward into the Indian Ocean via the Tasman outflow. This “supergyre” is an extension to include the South Pacific Ocean of the one proposed by de Ruijter<sup>27</sup>, which was originally confined to only the South Atlantic and Indian basins.

Our water trajectories show a strong resemblance between the Conveyor pathways and the wind-driven circulation structure. The wind-forced ocean dynamics is primarily driven by wind stress curl through the Sverdrup balance for the interior ocean and through a balance between vorticity from lateral stress and planetary vorticity for the

western boundary currents. To gain insight into the part played by wind in the modelled Conveyor, we applied the Island Rule model of Godfrey<sup>28</sup> to the annual-mean wind field used to force our simulation (the ECMWF 1977-1988 derived monthly climatology). The spatial structure of the wind-driven circulation is smoother than the one produced by our ocean model. Nonetheless, the SH subtropical “supergyre” (Fig. 4a), resemble that associated to the Conveyor shown in Fig. 3.

The wind forces the formation of two frontal regions (the Subtropical and Sub Antarctic fronts, STF and SAF, respectively). These fronts coincide with the maximum positive wind-curl and the southern limit of the positive subtropical wind-curl for the STF and the SAF, respectively (Fig. 4b). The southern branch of the supergyre flows in between. This region forms a dynamical barrier to strong meridional exchanges. Only SO waters north of both fronts can penetrate easily to the subtropical region, and propagate northward. In the SH Atlantic sector, the STF expands without intercepting land. Hence, meridional exchanges are not made easier and less than 1 Sv of water flowing from Drake Passage to the North Atlantic enters directly the South Atlantic. The most important fraction of the connection to the North Atlantic must first flow eastward to the Indian Ocean. Then it can enter the South-East Indian Ocean (~3 Sv) where the STF borders on the South Tasman Rise and the Campbell Plateau, or the Pacific (~8 Sv) where it comes across the American continent.

The evidence of the participation of the SH “supergyre” in the Conveyor implies that the global THC adjusts to the remote wind forcing. Not only these winds together with tides provide a mean for the NADW to upwell and transform, they also organize the path of the THC return-flow; therefore, they affect the water masses that reach the North Atlantic to compensate for NADW formation and spreading, with the Tasman route as the largest conveyor for the freshest and densest waters. Thus, the SH wind

forcing is strongly related to heat and freshwater transport into the South Atlantic and ultimately to the dynamical regime and stability of the THC<sup>1,16</sup>. Hence, in a changing climate, trends of the SH winds could represent an additional process to which the THC is sensitive<sup>29</sup>.

<fd> Style tag for displayed matter (e.g. displayed equations:  $a + b = c$  (1)).

## Methods

### *The global ocean model*

The simulation we analyzed was run with the ORCA OGCM2<sup>16</sup>. The horizontal resolution is  $2^\circ$  in longitude and varies in latitude from  $0.5^\circ$  at the equator to  $2^\circ \cos(\phi)$  poleward of the tropics. There are 31 levels in the vertical, with the highest resolution (10 m) in the upper 150 meters. Lateral mixing occurs only along neutral surfaces, and vertical mixing is computed with a 1.5 turbulent closure scheme, which provides a low diffusivity in and below the thermocline ( $0.1 \text{ cm}^2 \text{ s}^{-1}$ ). The model is forced by a daily climatology of momentum, heat and fresh-water fluxes derived from the ECMWF 11-year (1979-1988) reanalyses (smoothed by an 11-day running mean).

The experiment was designed for the recovery and study of the dynamics associated with the observed global ocean hydrology. Our analyses focus on the last year of a 10-year simulation run after addition to the model equations of a restoring term to the observed ocean temperature and salinity climatology<sup>16</sup>. The relaxation time-scale is 50 days in the upper 800 m and 1 year in the deep ocean. To let the model physics recover the boundary and equatorial currents not well resolved in the Levitus' climatology, this restoring term acts everywhere, except in the tropics, the surface boundary layer, and a 1000 km neighbourhood of the coastal boundaries. The computed transports compare well with observations (cf. discussion in *Blanke et al.*<sup>17</sup>)

### *The quantitative Lagrangian diagnostic*

The most natural way to estimate flow origins, pathways and the associated heat and freshwater transport is to follow the movement of water masses and diagnose their transformation<sup>5</sup>. To date, observations are too sparse in space and time to obtain a robust Lagrangian view of the global Conveyor. On the other hand, OGCMs provide coherent 3-D dynamical and thermodynamical fields.

Over the past years we developed a quantitative Lagrangian methodology to calculate in OGCMs large-scale interbasin connections and related pathways and water-mass conversions<sup>17</sup>. An equivalent approach is used here to reconstruct the global Conveyor, *i.e.*, the oceanic pathways that bring waters to the North Atlantic and export them after deep-water formation.

We computed the pathways associated with the modelled North Atlantic overturning. In our quantitative Lagrangian approach, water masses are represented by hundreds of thousands of elementary water parcels distributed over a given initial geographical section. We computed, backward in time, the trajectories of the parcels that represent the southward flow of NADW at 44°N in the North Atlantic (*i.e.*, characterized by a potential density anomaly greater than 27.7 kg m<sup>-3</sup>). These parcels originate in the downwelling of surface or subsurface waters that enter the North Atlantic either northward at 44°N or northward at the Bering Strait from the Pacific Ocean. The reconstruction of the THC in the rest of the ocean is obtained by integrating the same set of trajectories forward in time from 44°N. The Lagrangian computations used monthly varying velocity fields, and the results are presented as annual mean values.

<received> Style tag for received and accepted dates (omit if these are unknown).

1. S. Rahmstorf, *Nature*, **419**, 207 (2002)
2. S. Rahmstorf, In: *Encyclopedia of Quaternary Sciences*, Edited by S. A. Elias. Elsevier, Amsterdam (2006).
3. A. L. Gordon, *J. Geophys. Res.*, **91**, 5037, (1986).
4. W. J. J. Schmitz, *Reviews of Geophysics*, **33**, 151 (1995).
5. C. Wunsch, *Science*, **298**, 1179 (2002).
6. W. S. Broecker, *Natural History Magazine*, **47**, 79 (1987).
7. B. M. Sloyan, S. R. Rintoul, *J. Phys. Oceanogr.*, **31**, 1005 (2001).
8. R. Knutti, J. Flückiger, T.F. Stocker, A. Timmermann, *Nature* **430**, 851 (2004).
9. J. R. Toggweiler, J. B. Samuels, *Deep-Sea Res.*, **42**, 477 (1995).
10. W. Munk, C. Wunsch, *Deep-Sea Res.*, **45**, 1976 (1998).
11. F. Paparella, W. R. Young, *J. Fluid Mech.*, **466**, 205 (2002).
12. D. J. Webb, N. Sugimotohara, *Nature*, **409**, 37 (2001).
13. K. Döös, A. Coward, *WOCE Newsletter*, **27**, 3 (1997).
14. S. R. Rintoul, C. W. Hughes, D. Olbers In: *Ocean Circulation and Climate* (eds. G. Siedler, J. Church, and J. Gould). Academic Press, New York, 271 (2001).
15. Weijer, W., W. P. M. De Ruijter, H. A. Dijkstra and P. J. van Leeuwen, *J. Phys. Oceanogr.*, **29**, 2266 (1999).
16. G. Madec, M. Imbard, *Climate Dynamics*, **12**, 381 (1996).
17. Blanke, M. Arhan, S. Speich, G. Madec, *J. Phys. Oceanogr.*, **29**, 2753 (1999).
18. S. R. Rintoul, S. Sokolov, *J. Geophys. Res.*, **106**, 2815 (2001).
19. S. S. Drijfhout, J.M.H. Donners, W.P.M. de Ruijter, *Geophys. Res. Lett.*, **32**, doi:10.1029/2004GL021851 (2005).

20. M. Ollittraut (2007).
21. A. Ganachaud, C. Wunsch, *Nature*, **408**, 453 (2000).
22. M.-H. Rio, F. Hernandez, *J. Geophys. Res.*, **109**, C12032, doi:10.1029/2003JC002226 (2004).
23. N. A. Maximenko, P.P. Niiler, In N. Saxena (Ed.) *Recent Advances in Marine Science and Technology*, Honolulu: PACON International. 55, (2005).
24. N. Metzl, B. Moore, A. L. Poisson, *Paleoceanogr., Paleoclim., Paleoecolo.*, **89**, 81 (1990).
25. Y. You, *J. Geophys. Res.*, **103**, 30,941 (1998).
26. R. E. Davis, *J. Phys. Oceanogr.*, **35**, 683 (2005).
27. W. De Ruijter, *J. Phys. Oceanogr.*, **12**, 361 (1982).
28. J. S. Godfrey *Astrophys. Fluid Dyn.*, **45**, 89 (1989).
29. W. Cai, *Geophys. Res. Lett.*, **33**, doi:10.1029/2005GL024911 (2006).
30. A.H. Orsi, T. Whitworth III, W.D. Nowlin, *Deep-Sea Res. I*, **42**, 641 (1995).

#### Acknowledgments

We thank G. Madec and S. Drijfhout for fruitful discussions. This work was supported by the French Programme National pour l'Etude du Climat (SS and BB) and CSIRO's Wealth from Oceans Flagship (WC).

Correspondence and requests for materials should be addressed to S.S. (e-mail: Sabrina.Speich@univ-brest.fr).

Figure 1. The global reconstructed Conveyor shown as median pathways between successive oceanic sections crossed by water parcels. The colours indicate the mean depth of the transfer between two given sections. The North Atlantic overturning is defined here as the thermocline waters (in orange, red

and pink) transformed into NADW (blue) in the North Atlantic sector. Pathways show the upper and lower branches of the Conveyor. Numbers quantify the mass transfers between successive control sections (the Atlantic Equator, the Drake Passage, the SO section south of Australia and the Indonesian Throughflow). The transports are expressed in Sverdrups ( $1 \text{ Sv} = 10^6 \text{ m s}^{-1}$ ).

Figure 2. Binned transport of the northward-transmitted warm waters to the equatorial Atlantic with origins in the Indonesian Throughflow (red), the Drake Passage (green) and the Tasman outflow at  $145^\circ\text{E}$  (blue). The result is expressed as a function of salinity (upper panel), temperature (middle panel) and density anomaly (lower panel), at the origins (dashed lines) and on the equator in the Atlantic (solid lines). Though being originally slightly saltier, warmer and lighter than Drake Passage waters that are directly transmitted to the Atlantic without entering the Pacific, the Tasman outflow turns out to convey the greatest amount of fresh and dense water once it reaches the equatorial Atlantic.

Figure 3. Horizontal streamfunction  $\psi$  of the vertically-integrated transport accounted by the upper ocean waters transmitted northward to the North Atlantic, with origins in Drake Passage or in the same section in the North Atlantic but with a greater density. Contour interval is 1 Sv, and  $\psi$  is set to 0 over Africa. The pattern reveals the horizontal view of the upper branch of the global Conveyor. All the large-scale wind-driven structures of the ocean circulation emerge. This suggests that the wind plays a significant role in structuring the Conveyor. In particular, the South Atlantic, South Indian and South Pacific subtropical gyres are intimately connected: 3 Sv of upper branch water wrap around the three local gyres.

Figure 4. a) Transport streamfunction calculated with the Island Rule model of Godfrey<sup>28</sup> forced by the annual average of the ECMWF 11-year wind-stress climatology. Contour interval is 5 Sv. b) Wind stress curl ( $\text{N m}^{-3}$ , scaled by a factor  $10^{-7}$ ) for the ECMWF 11-year annual mean climatology. The location of the ACC fronts given by Orsi et al.<sup>30</sup> are superimposed: Subtropical front in magenta, Sub Antarctic in red, and Polar in black. Differences in position between the oceanic fronts and the maximum wind-curl and zero-curl lines likely result from the influence of the local bathymetry on ocean circulation and from the bias towards SH summer values of the hydrological data used<sup>30</sup>. Because of the spatial distribution of winds, and in particular of the SH positive subtropical wind-curl that encroach on the SO, well south of Africa and Oceania, an oceanic three-basin-wide supergyre cell stands out. Such a wide wind-driven cell has important consequences on the Conveyor paths and associated water masses along the paths, and thus on the role of the global ocean in the evolution of Earth's climate.

# Lagrangian reconstruction of the global Thermohaline Circulation

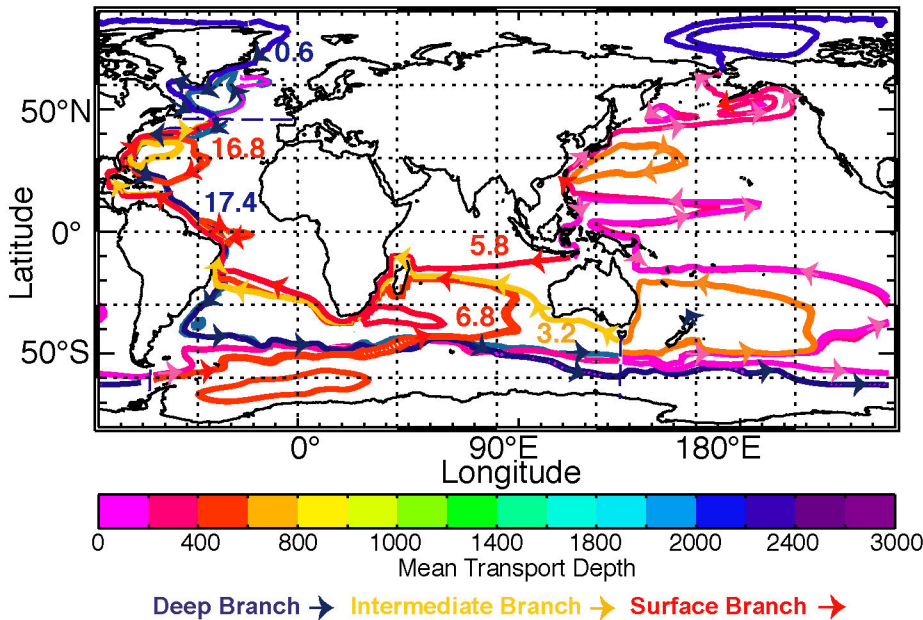


Figure 1

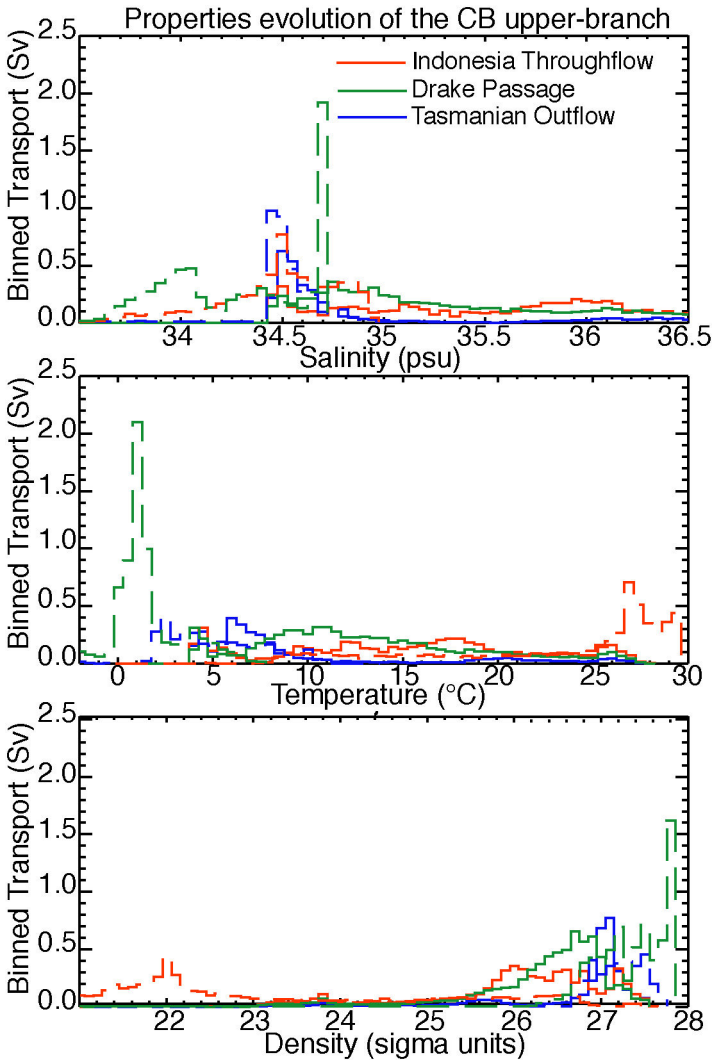


Figure 2

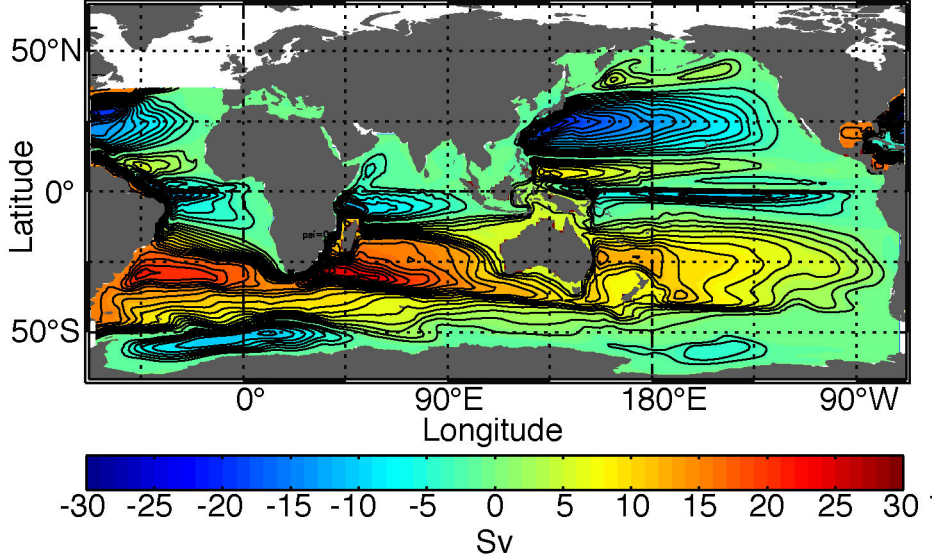


Figure 3

### ECMWF Wind forced Stream Function

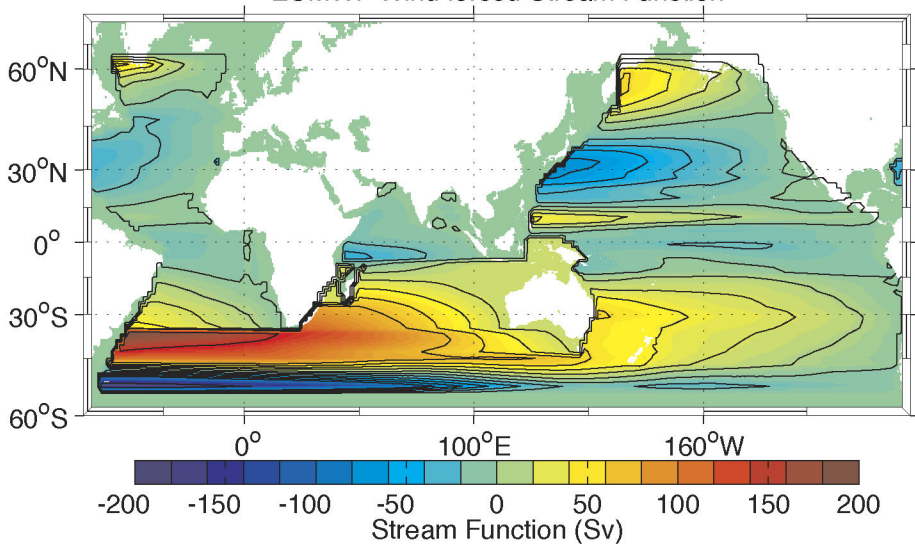


Figure 4a

b

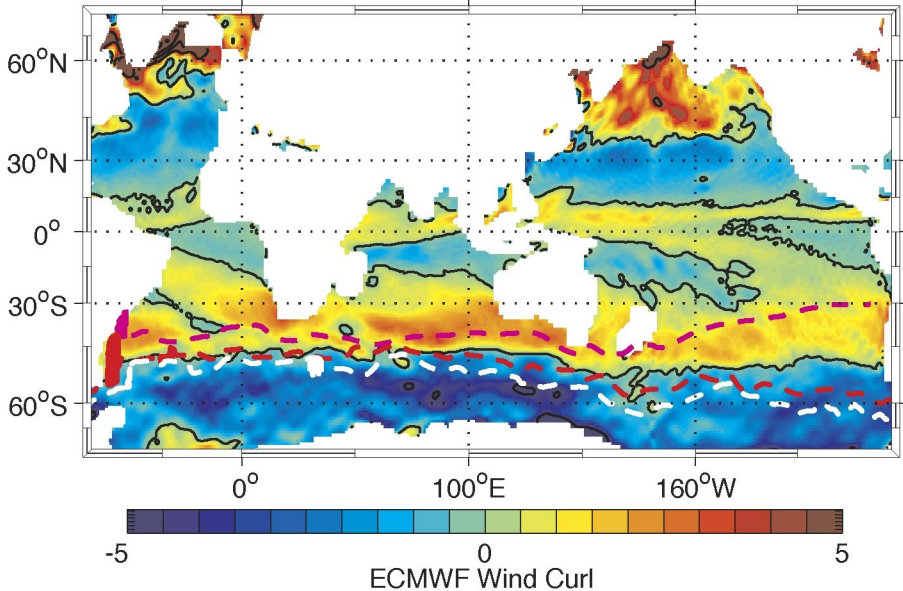


Figure 4b